

Schottky barrier engineering in III-V nitrides via the piezoelectric effect

E. T. Yu,^{a)} X. Z. Dang, L. S. Yu, D. Qiao, P. M. Asbeck, and S. S. Lau

Department of Electrical and Computer Engineering, University of California at San Diego, La Jolla, California 92093-0407

G. J. Sullivan

Rockwell International Science Center, Thousand Oaks, California 91358

K. S. Boutros and J. M. Redwing

Epitronics/ATMI, Phoenix, Arizona 85027-2726

(Received 6 April 1998; accepted for publication 25 July 1998)

A method for enhancing effective Schottky barrier heights in III-V nitride heterostructures based on the piezoelectric effect is proposed, demonstrated, and analyzed. Two-layer $\text{GaN}/\text{Al}_x\text{Ga}_{1-x}\text{N}$ barriers within heterostructure field-effect transistor epitaxial layer structures are shown to possess significantly larger effective barrier heights than those for $\text{Al}_x\text{Ga}_{1-x}\text{N}$, and the influence of composition, doping, and layer thicknesses is assessed. A $\text{GaN}/\text{Al}_{0.25}\text{Ga}_{0.75}\text{N}$ barrier structure optimized for heterojunction field-effect transistors is shown to yield a barrier height enhancement of 0.37 V over that for $\text{Al}_{0.25}\text{Ga}_{0.75}\text{N}$. Corresponding reductions in forward-bias current and reverse-bias leakage are observed in current-voltage measurements performed on Schottky diodes.

© 1998 American Institute of Physics. [S0003-6951(98)03939-4]

III-V nitride heterostructure field-effect transistors (HFETs) have emerged as highly attractive candidates for high-voltage, high-power operation at microwave frequencies.¹⁻⁵ A number of recent studies have demonstrated that the piezoelectric effect plays a key role in governing carrier distributions and other electronic properties in HFETs and other III-V nitride heterostructure devices.⁶⁻⁹ In particular, the piezoelectric effect is largely responsible for the extraordinarily high sheet carrier densities that can be achieved in the channel of a $\text{GaN}/\text{Al}_x\text{Ga}_{1-x}\text{N}$ HFET.^{7,8}

In this letter, we describe the design, experimental characterization, and analysis of $\text{GaN}/\text{Al}_x\text{Ga}_{1-x}\text{N}$ HFET structures in which the piezoelectric effect is employed to achieve a marked enhancement of the effective Schottky barrier height. Specifically, a two-layer $\text{GaN}/\text{Al}_x\text{Ga}_{1-x}\text{N}$ barrier is employed, within which the piezoelectrically induced polarization charge acts to increase the barrier height for gate leakage current in the HFET. This can be accomplished with no increase in the barrier thickness, and consequently little if any change in gate capacitance, and with only a minor impact on carrier concentration in the channel. It is anticipated that this will allow gate currents to be significantly reduced in nitride HFETs with little penalty exacted in channel conductance, transconductance, and other device properties.

The epitaxial structures used in these experiments were grown on *c*-plane (0001) sapphire substrates by low-pressure metalorganic vapor phase epitaxy (MOVPE). For all samples, a 3 μm GaN buffer layer was deposited initially, followed by various $\text{GaN}/\text{Al}_x\text{Ga}_{1-x}\text{N}$ structures constituting the barrier in an HFET structure. A series of several $\text{GaN}/\text{Al}_x\text{Ga}_{1-x}\text{N}$ heterostructures, enumerated in Table I, was grown for these studies. Details of the epitaxial growth

procedures and conditions have been described elsewhere.¹⁰ Schottky diodes were fabricated using evaporated Ti/Al annealed at 650–750 °C to form large-area ohmic contacts to the HFET layers, and Ni to form Schottky contacts consisting typically of 320 μm diam dots. Capacitance–voltage (C – V) profiling was used to determine sheet carrier concentrations in these structures, and photoresponse measurements were used to determine effective Schottky barrier heights.¹¹ The influence of these parameters on device properties was confirmed in current–voltage (I – V) measurements performed on Schottky diodes.

Figure 1 shows schematic diagrams of the epitaxial layer structure, energy-band-edge profile, and electrostatic charge distributions for a conventional $\text{GaN}/\text{Al}_x\text{Ga}_{1-x}\text{N}$ HFET structure and for a structure incorporating a two-layer $\text{GaN}/\text{Al}_x\text{Ga}_{1-x}\text{N}$ barrier. As shown in Fig. 1(b), incorporation of a GaN layer at the top of the heterostructure increases the effective Schottky barrier height by allowing the negative piezoelectric charge at the top of the $\text{Al}_x\text{Ga}_{1-x}\text{N}$ layer to be positioned within the HFET barrier structure. This approach is analogous to the use of a thin p^+ layer at or near the metal–semiconductor interface of an *n*-type Schottky diode to increase the effective barrier height electrostatically.¹² In a

TABLE I. Schottky barrier structures and corresponding sheet carrier concentrations and effective Schottky barrier heights measured by C – V profiling and photoresponse, respectively.

Sample No.	Barrier structure	n_s (cm^{-2})	ϕ_B^{eff} (V)
1	250 Å $\text{Al}_{0.15}\text{Ga}_{0.85}\text{N}$	2.8×10^{12}	1.29 ± 0.05
2	150 Å $\text{GaN}/250$ Å $\text{Al}_{0.15}\text{Ga}_{0.85}\text{N}$	1.8×10^{12}	1.41 ± 0.05
3	300 Å $\text{Al}_{0.25}\text{Ga}_{0.75}\text{N}$	5.0×10^{12}	1.52 ± 0.05
4	75 Å $\text{GaN}/225$ Å $\text{Al}_{0.25}\text{Ga}_{0.75}\text{N}$	4.5×10^{12}	1.89 ± 0.05
5	300 Å $\text{Al}_{0.30}\text{Ga}_{0.70}\text{N}$	5.5×10^{12}	1.56 ± 0.05
6	75 Å $\text{GaN}/225$ Å $\text{Al}_{0.30}\text{Ga}_{0.70}\text{N}$	5.1×10^{12}	1.83 ± 0.05

^{a)}Electronic mail: ety@ece.ucsd.edu

III-V nitride HFET, epitaxial growth and compositional control allow the magnitude and position of the charge within the barrier to be controlled very precisely.

A straightforward electrostatic analysis of the epitaxial layer structure and corresponding charge distribution for the

structure shown in Fig. 1(b) may be used to obtain analytic expressions for the effective barrier height, ϕ_B^{eff} , and the sheet carrier concentration, n_s , in the two-dimensional electron gas (2DEG) at the lower GaN/Al_xGa_{1-x}N interface. The sheet carrier concentration given by such an analysis is

$$n_s = \frac{1}{e} \left(\frac{\sigma_{pz} - \left(\frac{\epsilon_{\text{AlGaN}}}{d_{\text{AlGaN}}} \right) (\phi_B^{\text{GaN}} + E_F/e - V) + \frac{eN_d d_{\text{AlGaN}}}{2} + \left(\frac{\epsilon_{\text{AlGaN}}}{\epsilon_{\text{GaN}}} \right) eN_d d_{\text{GaN}}}{1 + (\epsilon_{\text{AlGaN}}/\epsilon_{\text{GaN}})(d_{\text{GaN}}/d_{\text{AlGaN}})} \right), \quad (1)$$

where σ_{pz} is the piezoelectrically induced polarization charge density, ϵ_{GaN} and ϵ_{AlGaN} are the dielectric constants of GaN and Al_xGa_{1-x}N, respectively, ϕ_B^{GaN} is the GaN Schottky barrier height, E_F is the Fermi level (relative to the GaN conduction-band edge) at the lower GaN/Al_xGa_{1-x}N interface, d_{GaN} and d_{AlGaN} are the thicknesses of the GaN and Al_xGa_{1-x}N layers in the HFET barrier structure, N_d is the background dopant concentration in the Al_xGa_{1-x}N layer, and V is the bias voltage applied to the Schottky contact. We assume a value for σ_{pz} of $2.5 \times 10^{13} x_{\text{Al}} e/\text{cm}^2$.^{7,8} The background dopant concentration in GaN is assumed to be negligibly small in comparison to the other charge densities present. The effective barrier height shown in Fig. 1(b) is given by

$$\phi_B^{\text{eff}} = \frac{1}{e} \Delta E_c + \phi_B^{\text{GaN}} - V + \frac{e d_{\text{GaN}}}{\epsilon_{\text{GaN}}} (n_s - N_d d_{\text{AlGaN}}), \quad (2)$$

where ΔE_c is the conduction-band offset between GaN and Al_xGa_{1-x}N. Equation (2) implies that for a simple Al_xGa_{1-x}N barrier, the Schottky barrier height is given by $\phi_B^{\text{GaN}} + \Delta E_c$; this is consistent with direct measurements of Al_xGa_{1-x}N Schottky barrier heights.¹¹ Furthermore, ϕ_B^{eff} is a function of applied bias voltage; the measurements and cal-

culations shown here are for $V=0$. While clearly approximate, Eqs. (1) and (2) provide a sound fundamental basis for design and analysis of nitride Schottky barrier structures in our studies.

Figure 2(a) shows ϕ_B^{eff} as a function of d_{GaN} for the structure shown in Fig. 1(b) with a 250 Å Al_{0.15}Ga_{0.85}N layer, for various background dopant concentrations in the Al_{0.15}Ga_{0.85}N layer, calculated using Eqs. (1) and (2). Also shown are experimentally measured effective barrier heights for samples 1 and 2, taken from Table I. A clear enhancement of approximately 0.1 V in the effective barrier height is observed for sample 2, and calculations of ϕ_B^{eff} and n_s using values for N_d of 5×10^{17} – $1 \times 10^{18} \text{ cm}^{-3}$ are in close agreement with the experimentally measured values. The results shown in Fig. 2(a) indicate that a low background dopant concentration in the Al_xGa_{1-x}N layer is required to achieve the maximum increase in ϕ_B^{eff} over that for a simple Al_xGa_{1-x}N barrier.

To achieve optimum performance in a nitride HFET, one would ideally wish to maximize both the effective barrier height and the sheet carrier concentration in the channel while maintaining a fixed barrier thickness and, consequently, a nearly constant effective gate capacitance. The

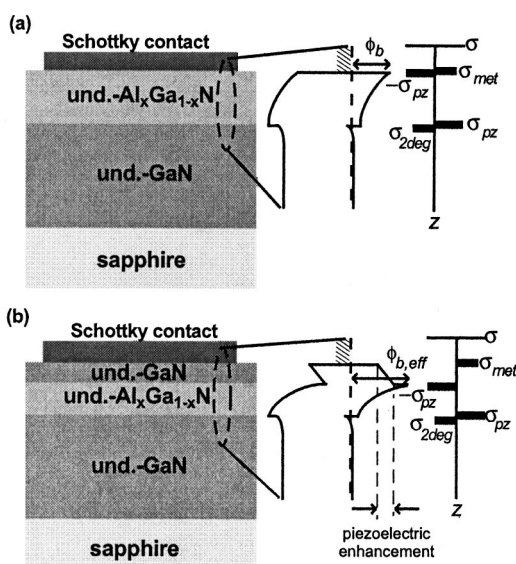


FIG. 1. Schematic diagram of epitaxial layer structure, band-edge energies, and electrostatic charge distributions for (a) a conventional GaN/Al_xGa_{1-x}N HFET structure and (b) an HFET structure incorporating a GaN/Al_xGa_{1-x}N two-layer barrier.

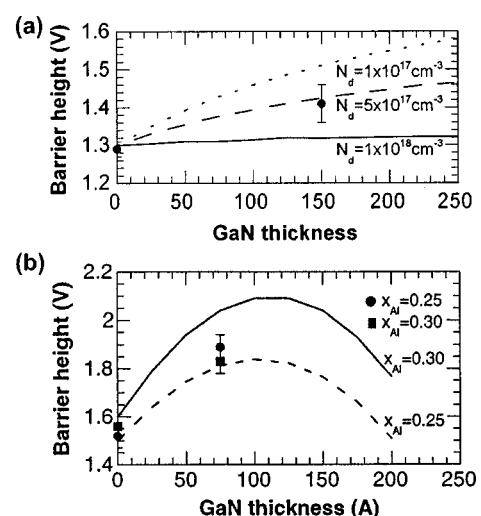


FIG. 2. (a) Effective Schottky barrier height ϕ_B^{eff} as a function of GaN layer thickness for a Schottky barrier structure consisting of 250 Å Al_{0.15}Ga_{0.85}N with a GaN cap. Lines represent calculated values; circles are measurements of ϕ_B^{eff} . (b) ϕ_B^{eff} for Schottky barrier structures consisting of GaN on Al_xGa_{1-x}N with a total barrier thickness of 300 Å. Circles and squares are measured values for $x_{\text{Al}} = 0.25$ and $x_{\text{Al}} = 0.30$, respectively.

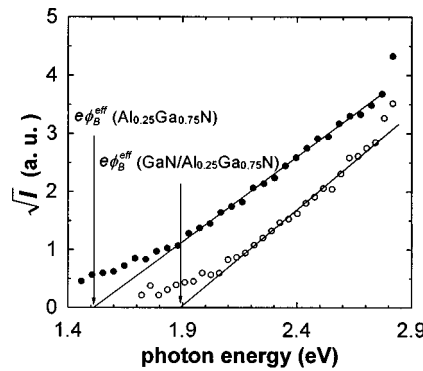


FIG. 3. Photocurrent per absorbed photon as a function of incident photon energy for a 300 Å $\text{Al}_{0.25}\text{Ga}_{0.75}\text{N}$ Schottky barrier structure and a 75 Å $\text{GaN}/225$ Å $\text{Al}_{0.25}\text{Ga}_{0.75}\text{N}$ barrier. A clear increase in effective Schottky barrier height is evident.

most effective mechanism for increasing ϕ_B^{eff} and n_s is to increase the Al concentration in the $\text{Al}_x\text{Ga}_{1-x}\text{N}$ layer. For a fixed total barrier thickness, however, the widths of the GaN and $\text{Al}_x\text{Ga}_{1-x}\text{N}$ layers must be chosen to yield the optimum combination of ϕ_B^{eff} and n_s . Figure 2(b) shows ϕ_B^{eff} calculated for a $\text{GaN}/\text{Al}_x\text{Ga}_{1-x}\text{N}$ barrier structure with a total thickness of 300 Å, as a function of d_{GaN} for $x_{\text{Al}}=0.25$ and $x_{\text{Al}}=0.30$. As shown in the figure, ϕ_B^{eff} reaches a maximum for $d_{\text{GaN}}=100-125$ Å and $d_{\text{AlGaN}}=175-200$ Å. However, from Eq. (1) one sees that n_s decreases with increasing d_{GaN} , necessitating a tradeoff between ϕ_B^{eff} and n_s in selecting an optimum value of d_{GaN} .

To achieve a large increase in ϕ_B^{eff} without an excessive reduction in n_s , 75 Å GaN/225 Å $\text{Al}_x\text{Ga}_{1-x}\text{N}$ Schottky barrier structures and 300 Å $\text{Al}_x\text{Ga}_{1-x}\text{N}$ control samples were fabricated (samples 3-6 in Table I). Figure 2(b) shows measured values of ϕ_B^{eff} for these structures, taken from Table I. A dramatic enhancement in ϕ_B^{eff} is observed when the top GaN layer is incorporated into the barrier structure; from Table I we see that this is achieved with relatively little reduction in n_s . Figure 3 shows photocurrent measured as a function of incident photon energy for a 300 Å $\text{Al}_{0.25}\text{Ga}_{0.75}\text{N}$ and a 75 Å GaN/225 Å $\text{Al}_{0.25}\text{Ga}_{0.75}\text{N}$ structure. For internal photoemission within the Schottky barrier structure, the threshold for nonzero photoresponse provides a direct measure of $e\phi_B^{\text{eff}}$. The data in Fig. 3 clearly demonstrate the large enhancement in Schottky barrier height created, via the piezoelectric effect, by the presence of the GaN cap layer. Figure 4 shows $I-V$ characteristics for samples 3 and 4. For the structure incorporating the 75 Å GaN cap layer, there is a clear reduction in current at forward bias voltages and a large suppression in reverse-bias leakage current, both of which we interpret as consequences of the increased effective Schottky barrier height. These features in the Schottky diode $I-V$ characteristics should translate directly into reduced gate leakage currents in III-V nitride HFETs.

In summary, we have proposed, experimentally demonstrated, and analyzed $\text{GaN}/\text{Al}_x\text{Ga}_{1-x}\text{N}$ HFET barrier struc-

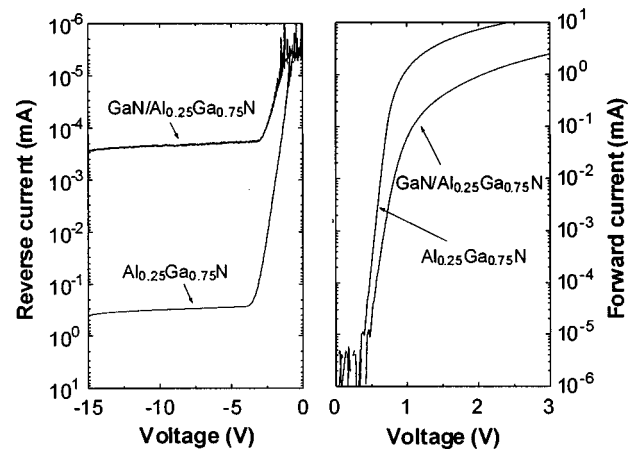


FIG. 4. Current-voltage characteristics for samples 3 and 4, demonstrating clear reductions in forward-bias current and in reverse-bias leakage current arising from the piezoelectric enhancement in Schottky barrier height for the structure incorporating a GaN cap layer.

tures in which the piezoelectric effect is exploited to achieve a large increase in effective Schottky barrier height compared to that for a simple $\text{Al}_x\text{Ga}_{1-x}\text{N}$ barrier. The influence of $\text{Al}_x\text{Ga}_{1-x}\text{N}$ composition, GaN and $\text{Al}_x\text{Ga}_{1-x}\text{N}$ layer thicknesses, and doping has been assessed. An optimized structure yielded an increase in effective barrier height of 0.37 V, with little penalty in sheet carrier concentration and barrier capacitance. $I-V$ characteristics of Schottky diodes confirm that the enhanced barrier height leads to substantial reductions in forward-bias current and reverse-bias leakage, suggesting that corresponding improvements in III-V nitride HFET performance should ensue.

The authors would like to acknowledge financial support from BMDO (Dr. Kepi Wu) monitored by USASMDC and contributions to sample growth by V. M. Phanse and R. P. Vaudo. One of the authors (E.T.Y.) would like to acknowledge financial support from the Alfred P. Sloan Foundation.

- 1 M. A. Khan, Q. Chen, M. S. Shur, B. T. McDermott, J. A. Higgins, J. Burn, W. J. Schaff, and L. F. Eastman, IEEE Electron Device Lett. **17**, 584 (1996).
- 2 A. Ozgur, W. Kim, Z. Fan, A. Botchkarev, A. Salvador, S. N. Mohammad, B. Sverdlov, and H. Morkoç, Electron. Lett. **31**, 1389 (1995).
- 3 Y. F. Wu, B. P. Keller, S. Keller, D. Kapolnek, P. Kozodoy, S. P. DenBaars, and U. K. Mishra, Appl. Phys. Lett. **69**, 1438 (1996).
- 4 S. C. Binari, J. M. Redwing, G. Kelner, and W. Kruppa, Electron. Lett. **33**, 242 (1997).
- 5 Q. Chen, J. W. Yang, R. Gaska, M. A. Khan, M. S. Shur, G. J. Sullivan, A. L. Sailor, J. A. Higgins, A. T. Ping, and I. Adesida, IEEE Electron Device Lett. **19**, 44 (1998).
- 6 A. Bykhovski, B. Gelmont, and M. Shur, J. Appl. Phys. **74**, 6734 (1993).
- 7 P. M. Asbeck, E. T. Yu, S. S. Lau, G. J. Sullivan, J. Van Hove, and J. M. Redwing, Electron. Lett. **33**, 1230 (1997).
- 8 E. T. Yu, G. J. Sullivan, P. M. Asbeck, C. D. Wang, D. Qiao, and S. S. Lau, Appl. Phys. Lett. **71**, 2794 (1997).
- 9 R. Gaska, J. W. Yang, A. D. Bykhovski, M. S. Shur, V. V. Kaminski, and S. M. Soloviov, Appl. Phys. Lett. **72**, 64 (1998).
- 10 J. M. Redwing, M. A. Tischler, J. S. Flynn, S. Elhamri, M. Ahoujja, R. S. Newrock, and W. C. Mitchel, Appl. Phys. Lett. **69**, 963 (1996).
- 11 L. S. Yu, Q. J. Xing, D. Qiao, S. S. Lau, K. S. Boutros, and J. M. Redwing (unpublished).
- 12 S. M. Sze, *Physics of Semiconductor Devices*, 2nd ed. (Wiley, New York, 1981), p. 293.